Simon Rauch (Autor)

Lateral emission characteristics of high-power broad-area lasers subject to external optical feedback

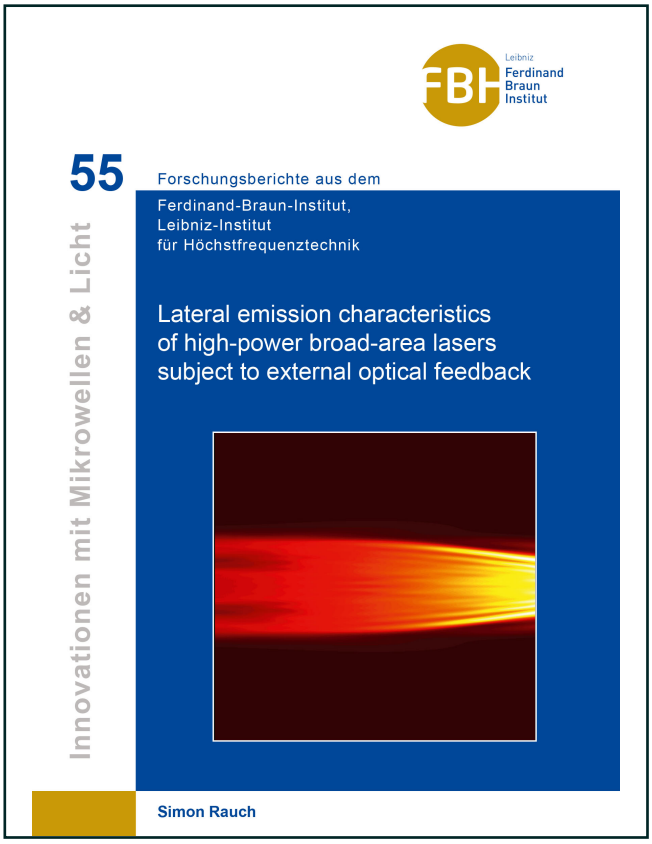

https://cuvillier.de/de/shop/publications/8185

1. Introduction

High-power broad-area laser diodes (BALs) are the most efficient devices to convert electrical into optical power [1]. Maximum peak efficiencies for free-running continuous-wave (CW) operation at room temperature reach over 70 % [2–5]. These extraordinary efficiency properties can be obtained with almost no penalty for wavelength stabilization of BALs by an external cavity (external-cavity BALs (EC-BALs)) that provides narrow-band optical feedback [6]. Such favorable characteristics along with their compact size and high integrability make BALs key components of efficient high-brightness solid-state lasers for materials processing. They are indispensable as pump sources for Yb-based fiber and disk lasers and as beam sources in high-brightness direct diode lasers. Prominent applications for such lasers are flat-sheet metal cutting and remote welding.

The widespread use of diode laser pump sources is due to their narrow-band, high-power radiation which has enabled room-temperature pumping of three-level solid-state lasers [7] that exhibit a low Stokes shift and hence low thermo-optical aberrations. Thereby inefficient lamp-pumped lasers have successively been replaced by diode-pumped solid state lasers (DPSSLs) during the last decade.
In 2017 Yb-doped DPSSLs had a 60 % market share of industrial lasers revenues [8]. This high position has evolved due to the fact that the broadband absorption band of several Yb-doped solids from around 900 nm to 950 nm overlaps with the emission spectral range of reliable high-power InGaAs/AlGaAs-based semiconductor lasers. As a consequence, Yb-doped gain media can be pumped by free-running BALs which allows compact and robust pump source architectures. Moreover, the close proximity of this broadband absorption band of Yb to the corresponding most widely used lasing transitions around 1030 nm and 1070 nm leads to a low quantum defect of less than 15 % and thus to a high optical-to-optical conversion efficiency.

Despite its high degree of sophistication, the technology of Yb-doped DPSSLs can be further optimized concerning efficiency with wavelength-stabilized EC-BALs. The latter may be used to pump the narrow-band zero-phonon transition of Yb-doped gain media close to a wavelength of 970 nm, which effectively reduces the remaining quantum defect to ∼6 %, when lasing around 1030 nm is assumed.

Disk lasers benefit especially from a reduction of the quantum defect by zero-phonon line pumping. Waste heat generated by the Stokes shift is the

dominant cause of beam quality deterioration, preventing single-mode output at multi-kW power levels [9]. Moreover, for Yb-doped fiber lasers, the pump light absorption is maximum for the zero-phonon line so that pumping at this wavelength helps to reduce the fiber length and hence to shift the onset of non-linearities like stimulated Brillouin and Raman scattering towards higher output powers [10].

By definition, DPSSLs exhibit a lossy conversion of pump to lasing photon. From a physical point of view, a direct diode laser that omits such a conversion process and uses the BAL light directly for materials processing, has the potential to become an even more efficient laser platform. Throughout the last 10 years, direct diode lasers, that are based on dense wavelength beam combining (DWBC) of hundreds of wavelength-stabilized EC-BALs into a single high-brightness output beam, have become feasible. The most promising technique in terms of brightness and robustness employs a single external grating-cavity that is simultaneously used for wavelength stabilization and beam combination [11, 12]. Most recent results demonstrate an electrical-to-optical (e-o) efficiency of 50 % at an output power of 2 kW [13], which is already close to the level of the most efficient fiber lasers [14], but still about 10 percentage points less than the efficiency of free-running BAL bars. This difference indicates that state-of-the-art direct diode lasers have the potential for further enhancement of e-o efficiency.

Despite the obvious physical advantages of employing EC-BALs for efficient high-power lasers, the industrial use of EC-BALs is problematic. The main technological challenge is that optical feedback accelerates long-term device degradation [15] and thus reduces the onset time for catastrophic optical damage (COD) [16]. As yet, these technological challenges outweigh the physical advantage of an improved efficiency.

Nearly all industrial high-power diode lasers are based on GaAs quantum well (QW) technology embedded in an index waveguide. This combination provides low optical and carrier losses along with nearly diffraction-limited beam quality in the vertical direction [17]. In order to meet industry lifetime requirements of several 10 kh, the design of high-power semiconductor lasers aims at keeping the optical intensity and the change of internal temperature as low as possible. Commonly, large longitudinal cavity lengths (3 to 6 mm) are employed to reduce thermal and electrical resistances. In order to balance the optical load, large vertical cavity designs with effective mode diameters in the order of 1 µm [18] or larger are used. Additionally, the output facets require supplementary passivation techniques since they are exposed to the highest intensities inside the laser and are susceptible to surface states of enhanced non-radiative recombination and absorption.

An additional characteristic of BALs is a wide lateral aperture (typically several 10 µm to several 100 µm), as illustrated in Fig. 1.1. The expansion of

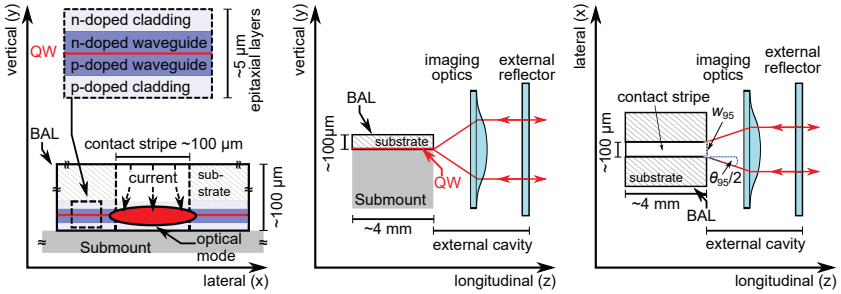

Fig. 1.1.: Profile views of a typical EC-BAL.

the lateral waveguide results in a further decrease of the thermal and electrical resistances and relaxes the optical load at the out-coupling mirror compared to fundamental-mode ridge-waveguide lasers with a typical lateral aperture size of $<10\,\mu m$. Because of that, the peak efficiency of state-of-the-art ridge-waveguide lasers is about 10 percentage points less than for BALs [19]. BALs manage to deliver output powers of 10 W and intensities of $\sim 10\,MW\,cm^{-2}$ reliably with an estimated mean time to failure of about 25 years [20]. However, the concept of broadening the lateral waveguide is always a trade-off between power and efficiency on one side and beam quality on the other side. For the wider the lateral waveguide, the more higher-order transverse-lateral modes are supported, degrading the beam quality as quantified by an increasing lateral beam parameter product (BPP_{lat}) [21, 22]. Here, BPP_{lat} is proportional to the product of lateral near- and far-field widths. Consequently, the lateral stripe width of BALs is chosen according to the required BPP_{lat} by a specific application. Furthermore, in the lateral direction, built-in index trenches close to the contact stripe lead to a far-field increase compared to gain-guided BALs [23]. This implies that, for a fixed aperture width, the lateral emission characteristics of gain-guided BALs are governed by thermal and carrier-induced refractive index changes.

Alternative approaches such as monolithic master-oscillator-power-amplifier configurations try to both circumvent multi-mode emission and relax the facet load by increasing and amplifying the fundamental mode from a ridge laser via a tapered amplifier section [24]. Based on such technology, output powers >5 W with nearly diffraction-limited beam quality have been demonstrated [25]. However, due to a comparatively large taper angle in the range of 6°, these devices exhibit an astigmatism that depends strongly on the operation current [26].

To utilize the advantages of a rectangular broad-stripe waveguide, but simultaneously avoid the mechanical complexity associated with an external

cavity design, monolithic alternatives to EC-BALs have been proposed. The most promising alternative approach is the distributed feedback (DFB)-BAL that employs intra-cavity etched Bragg gratings for wavelength stabilization. However, the etching process is rather complex and tends to introduce contamination and scattering losses [27]. As a consequence, the peak efficiencies of DFB-BALs are typically 5 to 10 percentage points lower compared to Fabry-Pérot BALs [28]. Moreover, the thermally induced spectral emission shift is about 50 times larger for DFB-BALs [29] compared to EC-BALs stabilized by thin-film filters [30] or diffraction gratings [11] and about 5 times larger than for EC-BALs stabilized by a volume Bragg grating (VBG) [31]. This is why only BALs that are stabilized externally are competitive for direct diode lasers based on DWBC.

The commercial success of BALs began with the application of double-clad fibers in 1988 [32] allowing efficient pumping of rare-earth doped fiber lasers and amplifiers with high-power multi-mode beams. In the beginning, primarily AlGaAs-based BALs in the 800-nm range were used for pumping Nd-based lasers and, later, InGaAs-based lasers in the 9xx-nm range for Yb. This transition resulted not only in a lower quantum defect, but also in a boost for reliability. It has been demonstrated that including indium in the quantum well increases the laser lifetime both in free-running [33] and external-feedback operation [34] by almost one order of magnitude.

At the end of the 1990s, the maximum CW power density before catastrophic optical mirror damage (COMD) was in the range of $18\,\mathrm{MW\,cm^{-2}}$ from a 100 µm-wide stripe. Steady improvement of facet protection technology [35–37] has lead to the situation that the maximum reported CW power amounts to $23.1\,\mathrm{MW\,cm^{-2}}$ [38] which was limited by thermal rollover instead of COMD.

In the 1990s, research on BALs mainly focused on understanding and mitigation of their multi-modal behavior and filamentation [39, 40] and accompanying non-thermal spatio-temporal instabilities [41–44]. The research was driven by the desire to restrict the high-power, multi-modal beam of BALs to fundamental-mode emission and simultaneously avoid or at least stabilize filamentation. In the early 2000s, external-cavity configurations using lateral fourier-space filtering seemed promising candidates to suppress higher-order transversal modes [45–48]. However, these approaches are always accompanied by a high efficiency loss and restricted to a narrow interval of operation – mostly close to threshold. This is due to the high semiconductor gain combined with self-heating induced waveguiding, commonly referred to as thermal lensing, helping high-order lateral modes to reach threshold.

In the following years, theoretical investigations of high-power semiconductor lasers [49–53] incorporated both thermally and carrier-induced refractive index changes and their respective impact on beam quality to investigate beam

quality deterioration with increasing output power [21, 54]. All applications have a certain limit of acceptable BPP_{lat}, which limits usable power extraction from BALs. However, limited quantitative agreement with experimental results made it difficult to identify the root causes of beam quality degradation unambiguously and quantitatively – which prompted additional experimental studies [23, 55].

In parallel but mostly independent of the investigations regarding beam quality degradation, extensive research on the dynamics of COD in laser diodes [56–61] was conducted, which, in case of sufficient cooling, represents the second main limitation of scaling the output power beside lateral beam quality deterioration. These studies on COD emphasize the importance of the temperature dependence of loss and thermal conductivities in order to reach the melting temperature of the active material and thus COD. Due to a detailed consideration of these computation-intensive thermal effects, most papers do not resolve the inputs for the thermal solver, carrier and photon distributions, in both lateral and longitudinal direction.

The past studies have revealed that increased BAL self-heating is a driving force for both beam quality deterioration and COD. However, for state-of-the-art InGaAs-based BALs in the 9xx-nm range, there is little known about the contribution of lateral-longitudinal variations of the internal temperature distribution to these two limitations. Especially, the analysis of EC-BALs requires exactly such a spatial resolution: The high load on the front facet is increased by light coupled back to the diode and potential mismatched parts of the feedback light strongly influence the temperature distribution locally [62].

The present thesis deals with the analysis and tailoring of the lateral beam parameters of EC-BALs as a function of the lateral-longitudinal internal temperature distribution. The analysis focuses on quasi gain-guided InGaAs-based BALs with a lateral stripe width of 100 to 140 µm that are usually used for fiber laser pumping and direct diode lasers.

In chapter 2, free-running operation and laser operation with matched optical feedback is considered. After a brief introduction of the employed experimental setup, laser structure and simulation tools, an analysis of the longitudinal temperature distribution follows: A simplified 2D lateral-vertical temperature solver is coupled slice-wise to the lateral-longitudinal carrier and photon profiles to estimate thermal lensing and its impact on near and far-field widths at both output facets (cf. sect. 2.4) of standard single-side outcoupling BALs. In section 2.5, two-side out-coupling by means of equal facet reflectivities is introduced as a means to tailor the lateral beam parameters, the temperature profile as well as lateral carrier accumulation. With this approach, the experimental feasibility of longitudinal intensity symmetrization by external optical feedback is analyzed subsequently.

In chapter 3, spatially mismatched feedback is investigated. The impact of absorption of feedback light by the adjacent layers surrounding the waveguide on facet heating and COD is studied in section 3.1. In the subsequent section, lateral displacement of the feedback return spot is discussed with respect to beam quality degradation.

The concluding chapter 4 provides an overview of the achievements of this thesis and a brief outlook for future investigations.

Parts of the present thesis have been published:

Journals

- S. Rauch, H. Wenzel, M. Radziunas, M. Haas, G. Tränkle, and H. Zimer, "Impact of longitudinal refractive index change on the near-field width of high-power broad-area diode lasers," *Applied Physics Letters*, vol. 110, no. 26, p. 263504, 2017.

- S. Rauch, C. Holly, and H. Zimer, "Catastrophic optical damage in 950-nm broad-area laser diodes due to misaligned optical feedback and injection" *IEEE Journal of Quantum Electronics*, vol. 54, pp. 1–7, Aug 2018.

Conference Proceedings

- S. Rauch, M. Haas, and H. Zimer, "Numerical and experimental investigation of near-field narrowing in broad-area laser diodes due to longitudinally asymmetric self-heating" in *2017 IEEE Photonics Conference (IPC)*, pp. 111–112, Oct 2017.

- S. Rauch, P. Modak, C. Holly, and H. Zimer, "Beam quality improvement of broad-area laser diodes by symmetric facet reflectivities," in *2018 IEEE International Semiconductor Laser Conference (ISLC)*, pp. 1–2, Sept 2018.

2. BALs subject to matched optical feedback

In this chapter the steady-state lateral-longitudinal temperature and intensity distributions of EC-BALs and their influence on the lateral beam parameters and lifetime is evaluated. Subsequently, a tailoring of the internal temperature and intensity profiles is conducted via facet reflectivity variation.

Regarding laser lifetime and reliability, the catastrophic optical (mirror) damage (CO(M)D) in the active zone of the semiconductor is the dominant thermally activated failure mode. Its temporal evolution can be subdivided into three phases, following the categorization by Hempel [60]: In the first phase, the potential damage volume is heated till it reaches a certain critical temperature (around 150 °C). Here, the time until the critical temperature is reached can vary from some nanoseconds during short-pulse current injection, to several years under CW operation. Once the critical temperature is reached, the second phase, the so-called thermal runaway sets in, in which the material heats up rapidly (on nanosecond timescale) beyond its melting temperature. In the melted area the epitaxial layer structure is destroyed and thus defects are created that spread during the third phase referred to as dark-line defects (DLDs).

Due to the ongoing industrial demand for high-power diode lasers with improved beam quality, the CO(M)D remains still a critical issue despite state-of-the-art facet passivation technology: Continuous defect accumulation during long-term degradation eventually ends in CO(M)D after a time period $t_{\mathrm{CO(M)D}}$ when the usable optical output power suddenly drops close to zero. Because of its thermal nature, $t_{\mathrm{CO(M)D}}$ can be expressed in terms of an Arrhenius law where the temperature can be considered proportional to the power per stripe width [63].

In fact, for each output facet, the lateral power confinement is quantified by the near-field width w_{95} which, along with the corresponding far-field width θ_{95}, determines $\mathrm{BPP}_{\mathrm{lat}}$ by [23]

$$\mathrm{BPP}_{\mathrm{lat}} = w_{95}\theta_{95}/4. \tag{2.1}$$

Here, the lateral beam parameters w_{95} and θ_{95} include 95 % power content (p.c.). This specific choice of power inclusion is arbitrary, but well-established in diode-laser industry.

Equation (2.1) indicates the dilemma between reliability and beam quality: While a larger near-field width is beneficial for laser lifetime, it increases

BPP_{lat} and thus reduces beam quality. Hence a compromise between BPP_{lat} and $t_{CO(M)D}$ has to be found for each application of BALs individually. In first approximation, w_{95} is determined and hence can be tailored by the contact stripe width w_c.

For gain-guided BALs at high-power operation, however, w_{95} can be significantly lower than w_c, which is referred to as near-field narrowing.

There is experimental indication [53, 64] that near-field narrowing is connected to a strong thermally induced lateral waveguide, often referred to as thermal lensing: As illustrated in Fig. 1.1, BALs are soldered with the epitaxial side down to the submount which is attached to a heat sink (not shown). Additionally, the lateral width of the contact stripe amounts to only about 2 % of the lateral submount width and to about 25 % of the vertical submount height. Hence, the waste heat, which is mainly generated in the active and waveguide layers within the area of the contact opening, spreads both in vertical and lateral direction towards the heat sink. As a major consequence of the lateral component of the heat flow, a thermally induced refractive index profile similar to a bell-shape builds up in the lateral direction.

So far, reported comparisons of experimental data of the lateral beam parameters with numerical simulations have either neglected longitudinal variations [65] or have restricted the benchmark to front-facet data only [53]. Yet in common single-side emitting BALs, the internal intensity distribution and hence the heat power density due to optical absorption are highly asymmetric with regard to the longitudinal direction [66]: Thermal lensing increases along the resonator towards the output facet. In particular, optical feedback changes the internal intensity by power re-injection and excitement of a different lateral mode set compared to the free-running operation [67]. These facts give a clear indication that the longitudinal temperature profile impacts the beam parameters θ_{95} and especially w_{95} differently for each facet and thus has to be considered for the estimation of $t_{CO(M)D}$.

Therefore, in this chapter the influence of the longitudinal temperature distribution on the beam parameters is investigated by means of numerical simulations in comparison with experimental results. Afterwards, w_{95} and hence BPP_{lat} are tailored by means of longitudinal intensity and temperature symmetrization.

2.1. Model of matched optical feedback

This section briefly introduces an idealization of optical feedback where perfect spatial and spectral back-coupling is assumed.

Figure 2.1 depicts the cavity model used for the analysis of BALs subject to optical feedback throughout this chapter. The laser system is modeled

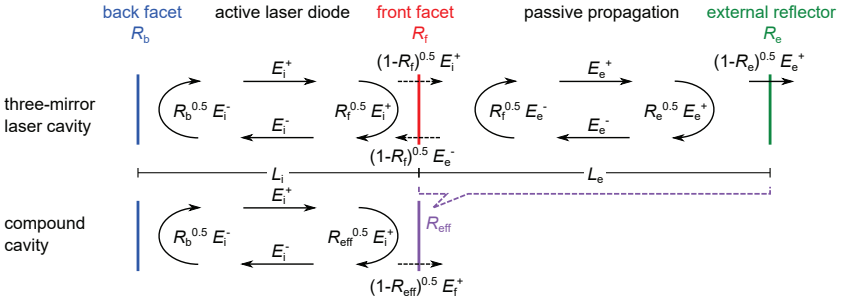

Fig. 2.1.: Three-mirror model for a Fabry-Pérot diode laser coupled to an external cavity via the front facet (top) and equivalent two-mirror system with an effective front-facet reflectivity R_{eff} (bottom).

via a simplified three-mirror system consisting of an internal active resonator of length L_i and an external passive cavity of length L_e. The forward and backward traveling electric fields of the internal resonator $E_\mathrm{i}^{\pm}$ and the external cavity $E_\mathrm{e}^{\pm}$ are coupled via the anti-reflection (AR)-coated laser front facet with a reflectivity of R_f. An external reflector returns a fraction, R_ext, of the BAL output power back towards the laser.

The back-coupling to the semiconductor waveguide can be quantified by the factor $\Gamma_\mathrm{c} = \eta_\mathrm{vert}\eta_\mathrm{lat}$, where η_vert and η_lat are the vertical (y) and lateral (x) coupling efficiencies, respectively. Due to strong vertical index guiding, η_vert can be expressed by the vertical overlap integral

$$\eta_\mathrm{vert} = \frac{\left|\int E_\mathrm{i}^{+} E_\mathrm{e}^{-}\,\mathrm{d}y\right|^2}{\int \left|E_\mathrm{i}^{+}\right|^2 \mathrm{d}y \int \left|E_\mathrm{e}^{-}\right|^2 \mathrm{d}y}. \tag{2.2}$$

Because of highly dynamic filamentation present in the lateral direction of BALs, it is more meaningful to estimate η_lat by the overlap of the time-averaged near and far-fields of emitted and re-entering intensity, assuming suitable (filamentation-free) analytical functions for the corresponding distributions, as done e.g. in [34]. For matched feedback, Γ_c is unity.

The fraction of back-coupled light reentering the laser can be derived by considering the external cavity as a Fabry-Pérot etalon with mirror reflectivities R_f and R_e. Based on this approximation, optical feedback from such an external cavity can be reduced to a single reflection of E_i^{+} at the front facet with an effective reflectivity R_eff (cf. Fig. 2.1, bottom). For the case of inco-

herent feedback, R_{eff} can then be derived from the phase-averaged reflectivity of a Fabry-Pérot etalon to [68]

$$R_{\mathrm{eff}} = \frac{R_{\mathrm{f}} + R_{\mathrm{e}} - 2R_{\mathrm{f}}R_{\mathrm{e}}}{1 - R_{\mathrm{f}}R_{\mathrm{e}}}. \tag{2.3}$$

Thereby the total fraction of the front-facet output power coupled back into the waveguide is given by $R_{\mathrm{eff}}\Gamma_{\mathrm{c}}$.

This compound cavity model automatically reduces the investigation of optical feedback to a steady-state analysis where all dynamics caused by the delayed back-coupling of feedback light, such as sub-microsecond spatio-temporal fluctuations, are neglected.

For spectral stabilization, R_{e} is chosen to have a narrow-band peak at the desired stabilization wavelength λ_{s} and the front facet is AR coated ($R_{\mathrm{f}} \ll R_{\mathrm{e}}(\lambda_{\mathrm{s}})$) so that, according to equation (2.3), $R_{\mathrm{eff}} \approx R_{\mathrm{e}}$ and the laser characteristics are dominated by the external cavity if $\lambda_{\mathrm{p}} = \lambda_{\mathrm{s}}$, with λ_{p} being the gain peak wavelength. In general, the threshold condition for lasing is that the total cavity losses consisting of internal absorption loss α_{i} and outcoupling loss $\alpha_{\mathrm{m}} = -1/(2L_{\mathrm{i}}) \ln (R_{\mathrm{b}}R_{\mathrm{eff}})$ are compensated by the modal gain g_{mod} averaged over the longitudinal (z) cavity length L_{i} [69]

$$\frac{1}{L_{\mathrm{i}}} \int_0^{L_{\mathrm{i}}} g_{\mathrm{mod}} \, \mathrm{d}z = \alpha_{\mathrm{i}} + \alpha_{\mathrm{m}}. \tag{2.4}$$

To understand the integration bounds, note that the right-handed coordinate system used throughout this thesis has its origin in the QW at the center of the contact stripe at the back facet. In case of a mismatch of the gain peak wavelength λ_{p} and λ_{s}, the resulting lasing wavelength λ_0 aligns to either of them according to which of the corresponding operation states exhibits the lowest injection current that fulfills equation (2.4). This current minimum is the lasing threshold current I_{th}.

The presented analysis in this chapter targets investigating the feedback impact on BALs without dispersion of R_{e}. Therefore, the peak reflectivity of the external reflector $R_{\mathrm{e}}(\lambda_{\mathrm{s}})$ is virtually extended to the full spectral range, effectively treating it as a constant.

An important consequence of the concept of matched feedback is, in particular, that free-running and external-cavity operation are equal for steady-state analyses. Within this framework, investigations based on the variation of facet reflectivities are valid for both operation modes alike. Yet dynamical phenomena such as feedback-induced lateral intensity modulation have to be analyzed by using a true coupled cavity.